THE JOURNAL OF PHYSICAL CHEMISTRY Letters

pubs.acs.org/JPCL Letter

Local Atomic Heat Currents and Classical Interference in Single-Molecule Heat Conduction

Renai Chen, Inon Sharony, and Abraham Nitzan*

Cite This: J. Phys. Chem. Lett. 2020, 11, 4261−4268 Read Online

ACCESS | Metrics & More | Article Recommendations

ABSTRACT: We consider interference effects in vibrational heat conduction across single-molecule junctions. Previous theoretical descriptions of such effects have relied on the quantum Landauer-type expression for heat transport by harmonic molecules, and such observations are sometimes termed "quantum interference". Here we demonstrate via classical atomistic simulations of heat conduction in benzenedithiol single-molecule junctions that the room-temperature effect is essentially classical. In fact, classical simulations and quantum evaluation of room-temperature heat conduction in these systems yield similar results. Simulations of para-, meta-, and ortho-connected benzenedithiols between gold substrates yield conductions in the order para > ortho > meta, which is similar to trends found in the electronic conduction of these structures. The (essentially classical) interference origin of this ordering is indicated by the similarity of the quantum and classical behaviors of these systems.

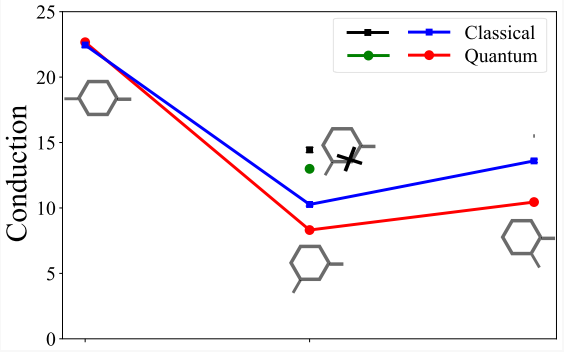

Heat conduction in molecular junctions has become a subject of increasing interest because of its fundamental role in transmitting and dissipating energy on the molecular scale as well as its technological importance in the performance and stability of envisioned molecular nanodevices.[1−9] The recent measurement of heat conduction in single-molecule junctions[10] demonstrates the impressive development of state-of-the-art microscopic thermal probing and measuring techniques and potentially opens the door to unveiling the interplay between molecular (and junction) structure and the ensuing thermal transport properties.

Quantum interference (QI) has been often reported to play a role, sometimes important, in molecular electronic conduction.[11−19] While nuclear motions (henceforth sometimes termed phonons) usually dominate molecular heat conduction,[5,7,20−25] calculations based on the quantum Landauer formula for heat conduction in the harmonic molecule limit indicate that interference may affect phononic thermal conduction as well, and these observations have been also termed quantum interference.[8,26] Figure 1 illustrates the main difference between electron and phonon transport in molecular junctions. First, the different statistics of these carriers implies different occupation distributions in the leads. Consequently, the corresponding transmission functions are sampled differently in the two cases and, in particular, electron transmission can be tailored to sample a narrower energy window thereby displaying interference effect on transport more prominently. The basic origin of interference in both cases is the spatial structure of the conducing orbital(s) in the electronic case or delocalized modes in the vibrational one that are both determined by atomic positions in the molecular bridge. For example, comparing commonly used tight binding models for electronic structure to harmonic atomic structures with nearest-neighbor interactions shows a close mathematical similarity that implies similar implications of geometrical structure to interference. Nonetheless, because phonons are classical waves, their dynamic properties are mostly determined by classical mechanics, and it may be expected that interference phenomena will show in classical phononic thermal transport.

In this Letter, we examine the vibrational heat conduction behavior of a benzene molecule connected to gold substrates via thiol bonds using classical molecular dynamics (MD) simulations with the full molecular force field as well as the quantum Landauer expression with harmonic part of the same force field. We focus on the conduction properties of para-, meta-, and ortho-connected rings and find considerable differences that can be traced to interference between different phonon-transfer pathways. Remarkably, at room temperature, the quantum and classical calculations yield qualitatively similar results. Both show similar trends that indicate interference

Received: February 12, 2020
Accepted: May 6, 2020
Published: May 6, 2020

https://dx.doi.org/10.1021/acs.jpclett.0c00471
J. Phys. Chem. Lett. 2020, 11, 4261−4268

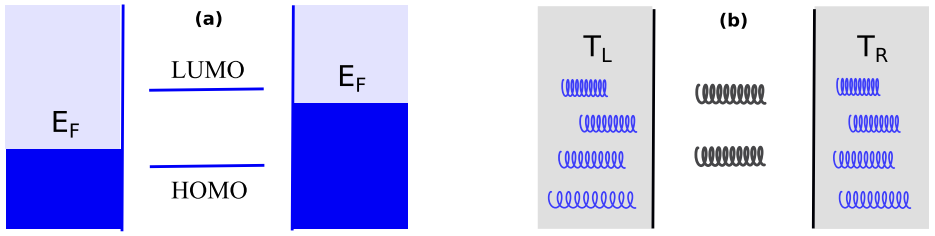

Figure 1. Schematic diagram of electron transport (a) and vibrational energy transfer (b) in molecular junctions.

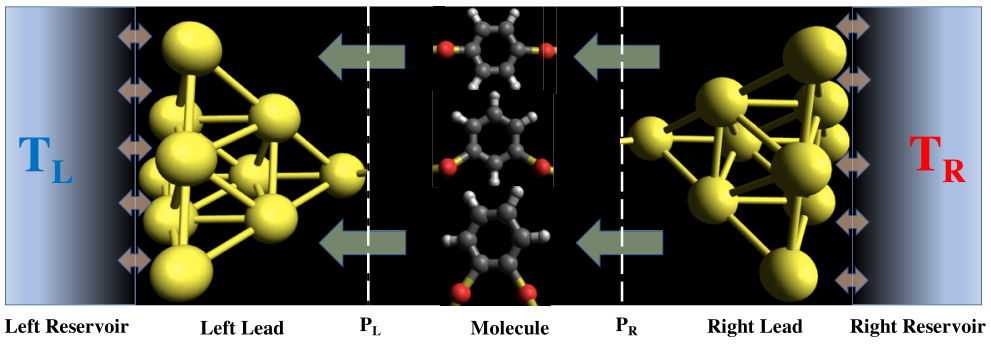

Figure 2. Artist representation of a typical system studied in this work. The unidiretional arrows across left plane (P_L) and right plane (P_R) denote the direction of heat flows. The double arrows show the connections between the exterior layer of gold lead to the thermal reservoirs, which are characterized with temperature T_L and T_R, respectively.

between conduction pathways when comparing the heat conduction properties of para, meta, and ortho benzenes.

The junction model used in the simulations comprises the molecule and the explicit leads that together form an extended inner system (referred to below as "extended molecule") and the thermal reservoirs (Figure 2). The explicit leads each have three layers of gold atoms in a cone-like structure (one, three, and nine gold atoms in the first, second and third layer, respectively) that mimics scanning tunneling microscope (STM) tips. The external reservoirs are equilibrium Markovian baths, characterized by specific temperatures (T_L and T_R) that represent the experimentally tuned macroscopic substrates. Unless otherwise stated, the friction associated with the coupling between the extended molecule and the external thermal reservoir is taken to be 1 ps^{-1}. The stochastic MD simulation is implemented using stochastic nonequilibrium Langevin dynamics by utilizing a customized GROningen MAchine for Chemical Simulations (GROMACS, currently version 4.5[27]) platform. The universal force field (UFF) of Rappe et al.[28] is employed for all the molecules in the study. The molecular system (together with the segments of the substrates embedded in the molecular subsystem to form an extended molecule) is first equilibrated to the average temperature of the thermal baths starting with its minimum energy configuration and then brought to a nonequilibrium steady state (SS) with the two leads kept at different temperatures. This part of the simulation is typically a few nanoseconds long. Once the SS is reached, thousands of production runs are used to get an ensemble of MD trajectories and forces needed for the steady-state heat currents.

The quantum Landauer-type calculations are done by using the harmonic part of the extended molecule force field to calculate the phonon transmission probability $\mathcal{T}(\omega)$. (An example, for room-temperature structures, is shown in the Appendix). The (phononic) heat current is obtained from the Landauer expression[7,29,30]

$$J = \frac{\hbar}{2\pi}\int_0^\infty \mathcal{T}(\omega)[f(\omega, T_L) - f(\omega, T_R)]\omega\, d\omega \quad (1)$$

Here f function is the Bose−Einstein distribution function which depends the temperature of the bath, $f(\omega, T) = (e^{\hbar\omega/k_B T} - 1)^{-1}$. Our implementation is achieved by incorporating GROMACS utilities into homemade code. From a high-level description, the Hessian (dynamical force matrix) of the molecular system is obtained, followed by its diagonalization in order to get the normal modes. The eigenstates of the modes are then used to calculate the basic quantities (e.g., self-energies, Green's function, *etc.*), which are used to evaluate $\mathcal{T}(\omega)$. Further details on technical aspects of these simulations are provided in ref 31.

We note that although the thermal properties of the external baths are affected by imposing Markovian dynamics (white noise) for the relaxation at the boundary between the explicitly addressed substrate segment and the outer thermal environment, this white noise is adequately filtered through the explicit substrate layers so that it acts on the molecule itself with the characteristic spectral density features of the simulated gold. Results obtained using this model to simulate heat conduction through alkanedithiol chains[31] show good agreement with experimental observations.[10] The fact that the filtered noise emphasizes the low-frequency regime is one reason why quantum and classical results about room temperature are qualitatively similar as shown below.

Because the classical simulation yields atomic positions, velocities, and forces along the simulated trajectories, it is evident that we can address not only the total steady-state heat current (phononic energy flux) carried by the molecule but also the energy flux associated with individual atoms. However, the procedure for doing this is not absolutely unique because to define energy currents involving individual atoms within the molecule we need first to define individual atomic energies, a task which is somewhat arbitrary for the potential energy because of its nonlocal nature. In ref 31 we have done so by assigning portions of the potential energy to individual atoms as

https://dx.doi.org/10.1021/acs.jpclett.0c00471
J. Phys. Chem. Lett. 2020, 11, 4261−4268

follows: First, identify different contributions to the potential energy associated with atom j as V_{jn} (n = 2, 3, ...) which are sums over all n-atom interaction terms in the molecular force field that involve this atom. A coarse-grained description of the energy distribution between the atoms is obtained by assigning to atom j the potential energy $\sum_n n^{-1}V_{jn}$. Once this choice is made, the force on the atom can be evaluated as well, and the rate of energy change for this atom is obtained as a product of this force and the atom speed. This leads to the energy current between two atoms, i and j, in the form $J_{ij} = \sum_n J_{n,ij}$ where[31,32]

$$J_{n,ij} = C_{n,j}\mathbf{f}_{n,i}\cdot\mathbf{v}_i - C_{n,i}\mathbf{f}_{n,j}\cdot\mathbf{v}_j \quad (2)$$

in which $\mathbf{f}_{n,j}$ is the force derived from interaction V_n with respect to the coordinate of atom j. (This choice, used to produce Figure 6, has no bearing on the heat conduction calculations shown in Figures 3−5.)

The simulated total heat conductance of the benzenedithiols in the three junctions is displayed in Figure 3. The steady-state heat current is calculated by summing up all the interatomic currents going through a plane perpendicular to the molecular chain, e.g., the current J_L and J_R through, respectively, the planes P_L and P_R in Figure 2, and averaging over time (after steady state was achieved) and trajectories. The resulting averaged J_L and J_R are found to be the same within 0.5%. The heat conductance is the ratio of this heat current and the temperature difference ΔT.

The nonmonotonic behavior seen in Figure 3 as the junction structures change from para to meta and ortho configurations obviously does not result from changing interactions, and the possibility that interference between energy fluxes propagating along different paths is the source of this behavior, analogous to similar observation of electronic conduction through these configurations,[14,19,34,35] suggests itself. Indeed, when one of the paths is blocked as shown in Figure 3 for the meta configuration, conduction increases. Simulations done under different conditions are consistent with this assessment. Figure 4 compares heat conduction for three different sets of temperature biases, using both MD simulations and Landauer's calculations.

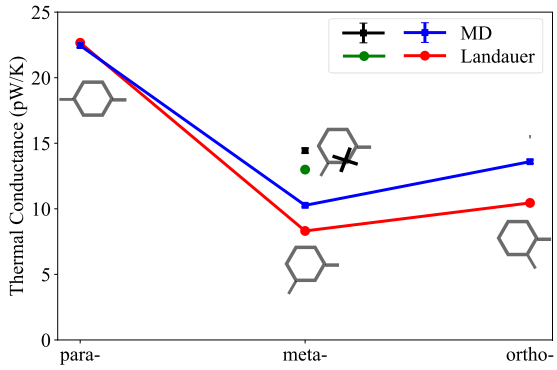

Figure 3. Thermal conductance of dithiolated-benzene molecules in gold−molecule−gold junctions with different connection (para, meta, and ortho) configurations. Shown are results from classical MD simulations and from the quantum Landauer's formula. The error bars represent standard errors (= standard deviation/square root of the sample size, which is a statistical uncertainty indicator of the estimated mean value of the conducted measurements[33]). The green and black dots represent the conduction calculated using the Landauer formula and classical MD simulations, respectively, for the meta configuration in which heat transport through the site marked X is blocked by taking the mass to be artificially large (100 carbon atom mass).

Panel a shows the same results as Figure 3, while panels b and c show results for high (600 and 650 K) and low (10 K and 60 K) temperatures, respectively. Figure 5 examines the effect of disorder, comparing the para and meta signals from the original molecule, and from a similar molecule in which a single hydrogen atom is replaced by a fluorine atom. The following observations can be made:

(a) While interference is seen also in the higher-temperature simulations (Figure 4b), the difference between the conductions of the para, meta, and ortho configurations is smaller at this higher temperature.

(b) The classical simulations and the Landauer formula results are closer to each other at room temperature (Figure 4a) than at 600 K (Figure 4b). The reason may be that the Landauer results are obtained for a molecular model described only by the harmonic part of the full potential. Errors in this approximation become more pronounced at higher temperatures where the system explores more of the anharmonic part of its force field.

(c) Although the physical distance between the contact is smaller in the ortho and meta configurations, the total heat current appears to be highest in the para-connected structure, where the thermal contacts are physically furthest from each other. Such a counterintuitive heatmap can again be taken as an indication of the interference effect.

(d) At low temperature (Figure 4b) we see that the quantum result deviates strongly from the classical calculation. Remarkably the interference pattern all but disappears. At such low temperature only very low-frequency modes contribute to the transport, more so in the quantum calculation. Such modes usually involve motions of many atoms so that "transport paths" become less distinct, quenching interference between paths.

(e) Introducing an impurity atom into the system has a strong effect on path interference, as is seen in Figure 5. In particular, the destructive interference that characterizes the meta structure is strongly reduced by such impurity even if it involves a substitution of an hydrogen atom that by itself does not make a large effect on the phonon transmission (however substitution by fluorine does).

A cautionary note is in order. While the configurations studied appear to be molecular analogues of a double-slit system where phonon amplitudes propagating along different paths interfere, the actual situation is more involved, as can be seen by looking at real-space steady-state atomic heat flows in these junctions. Figure 6 shows local heat fluxes obtained from eq 2, indicating their direction and magnitudes by arrows of various thicknesses. These currents take place between each atom pair, although they are naturally higher between nearest neighbors. It should be emphasized that, while partial cancellation between currents going in (partly) opposite directions gives rise to some of the observed trends in Figure 3 and 4, interference is also manifested in the velocities of and total forces experienced by individual atoms, an effect not seen in this figure. The total heat currents express a complex interplay between these forces and velocities that eventually results in these current maps.

Furthermore, it should be kept in mind that interference is, to a large extent, a matter of representation. In a harmonic junction heat is carried independently by the system normal modes, and in the normal mode represetation interference between different propagation paths translates into transmission properties of

https://dx.doi.org/10.1021/acs.jpclett.0c00471
J. Phys. Chem. Lett. 2020, 11, 4261−4268

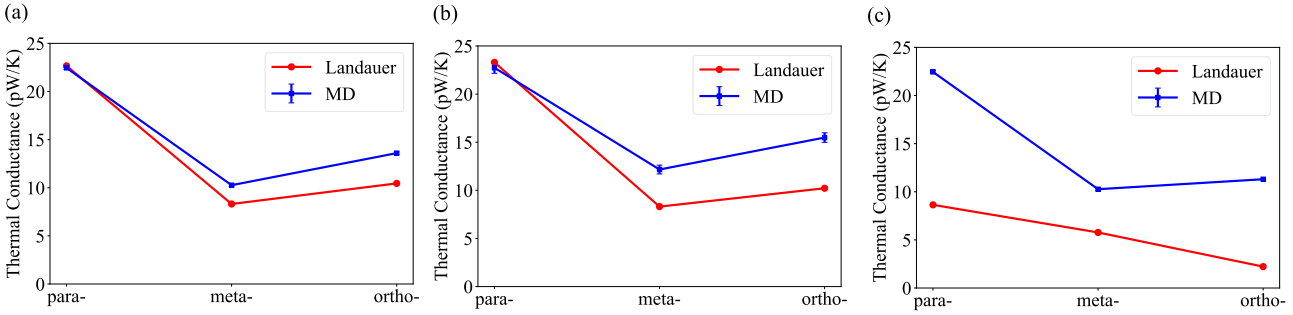

Figure 4. Thermal conductance for para-, meta-, and ortho-benzenedithiol molecules, calculated from classical MD simulations and from the Landauer expression under different temperatures: (a) T_{hot} = 350 K and T_{cold} = 300 K; (b) T_{hot} = 650 and T_{cold} = 600 K; (c) T_{hot} = 60 and T_{cold} = 10 K. The error bars for MD represent standard errors (as in Figure 3).

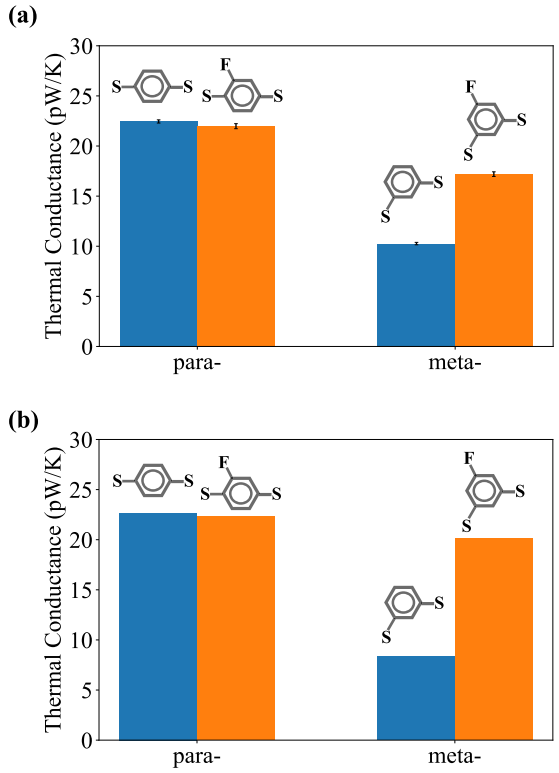

Figure 5. Thermal conductance for para- and meta-benzenedithiol molecules, simulated for the configurations with and without replacing one hydrogen with one fluorine at the position indicated in the molecular diagram, for the temperature bias of 300−350 K. Panels a and b show results from MD and Landauer calculations, respectively. The error bars in panel a represent standard errors (see caption of Figure 3).

individual nodes, e.g., a node assumed by a mode at the molecule-lead bond which will render this mode unable to contribute significantly to the heat conduction process. Figure 7 demonstrates this point by showing the frequency-resolved classical transmission. It is generated as follows: We consider just the benzenedithiol species, use the harmonic part of the molecular force field, and focus on the two sulfur atoms. One sulfur atom (say, atom 12 in Figure 6a) is driven by a periodic force that makes its coordinate (deviation from equilibrium) oscillate with frequency ω. A friction γ is applied to the motion of the other sulfur atom (atom 11 in Figure 6a), thus forming a driven−damped harmonic system (see Appendix). At steady state there is a constant heat flux $J(\omega) = \sum_j \gamma_j \langle \dot{x}_j \rangle^2$, where the sum is over directions in the local coordinate system that defines the deviation of atom 11 from its equilibrium position. This flux represents the heat transmission spectrum of the unbound molecular species itself and is plotted against the driving frequency ω in Figure 7. The result depends on the relative magnitudes of the frictions γ_j, and in the simulations shown in Figure 7 we have assumed that the friction is dominated by the motion along the S−C bond, which in the full simulations shown in Figures 3 and 4 correspond to a direction nearly perpendicular to the gold substrate. The integrals of these spectra $I(\omega) = \int_0^\omega d\omega J(\omega)$ are shown as functions of ω in Figure 8, showing a trend similar to that observed in Figures 3 and 4.

These results, which lack information about molecule−leads binding and lead spectral function, as well as mode populations, do not directly apply to the actual heat-transfer process, but they provide insight into the meaning of interference. Obviously, when the calculated transport is resolved to emphasize the contribution of different normal modes to the overall transmission, the "interference" concept is not necessarily useful. It becomes useful when we develop understanding of transport along individual spatial paths; we then observe that opening a path may reduce transport rather than increase it, as was seen in Figure 3, or more generally, that transport in a system comprising several paths is not a simple sum over individual paths. The fact that this interference has a classical origin is not surprising given the nature of phonons as traveling waves.

In summary, we have computationally analyzed the heat conduction properties of benzenedithiol-based single-molecule junctions with different bridging configurations using both classical MD simulations and quantum Landauer's calculations. Our results indicate that the harmonic representation (used in the quantum calculations) as well as quantum effects (neglected in the classical calculation) are of secondary importance for such junctions at room temperature. Interesting deviations between the two calculations are found at low temperatures (where classical mechanics fails) and higher temperatures (where the harmonic approximation, used in the quantum calculation, fails). Comparing heat conduction trends between para-, meta-, and ortho-connected molecules shows strong indications of the role played by interference between different energy flow paths. This interference persists in the classical calculation, indicating its classical origin. We have examined the manifestation of this phenomenon when examined with frequency resolution and have pointed out that in the normal mode basis path interference translates into transmission properties of individual normal modes. It will be interesting to explore these types of behaviors further, to discern quantum from classical effects and to

https://dx.doi.org/10.1021/acs.jpclett.0c00471
J. Phys. Chem. Lett. 2020, 11, 4261−4268

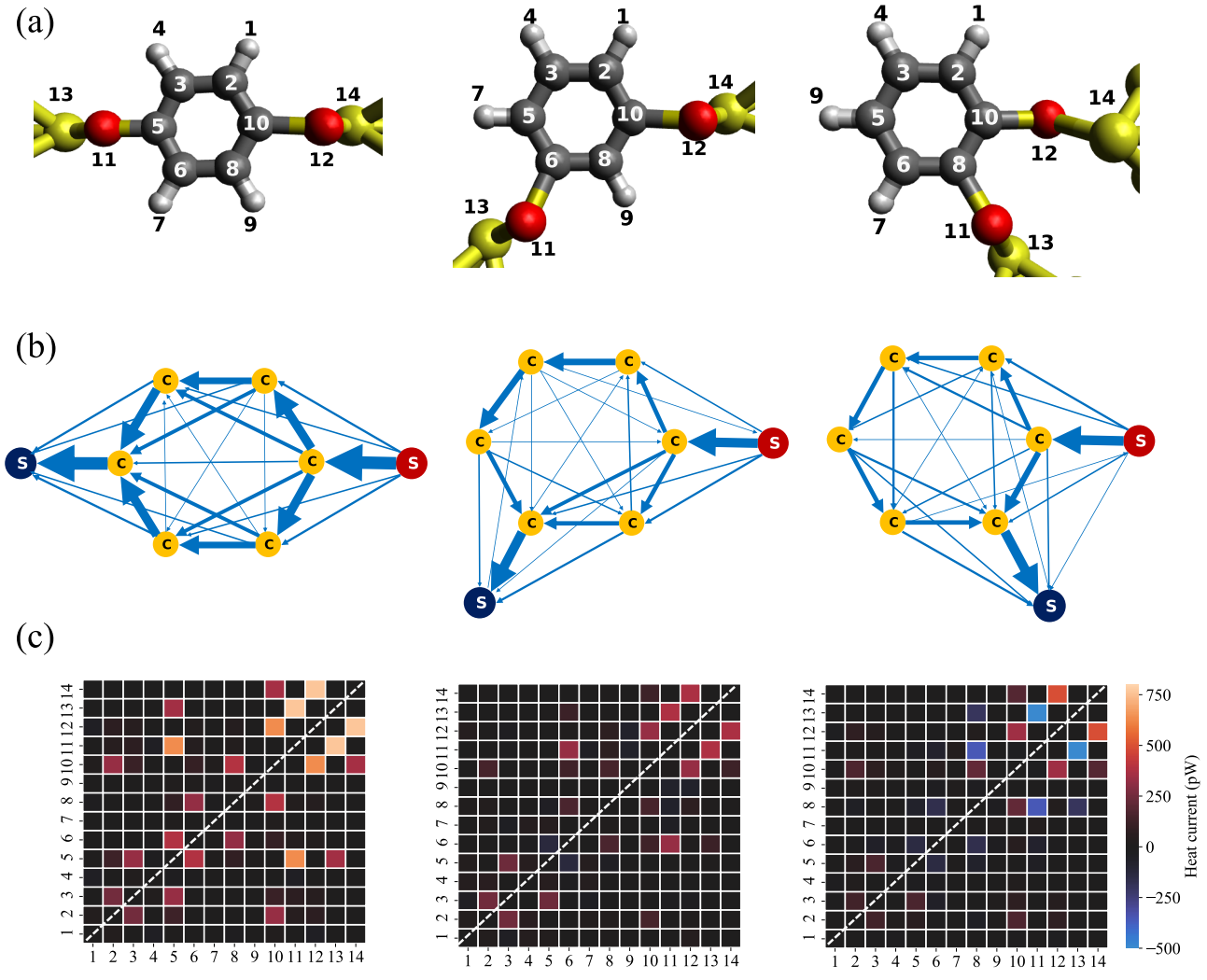

Figure 6. Heat current maps in junctions comprising benzene molecules connecting in (from left to right) para, meta, and ortho configurations between gold substrates, computed by MD simulations at steady state under temperature bias of 300 and 350 K on the two sides of the junction. (a) Molecular structures indicating atom numbering that is used in panel c. Small light gray balls, bigger dark gray balls, red balls, and yellow balls represent hydrogen, carbon, sulfur, and gold atoms, respectively. (b) A map of local heat currents calculated at steady state for the three junction configurations. Arrows and thickness correspond to directions and magnitudes of the local currents. (c) A two-dimensional map of local currents between atoms arranged according to the numbering shown in panel a. Current direction is here indicated by sign: positive corresponds to leftward or leftward-tilted flux, or for vertical flow (for example between atom 3 and 6) to upward flux. Note that the heat current maps shown in panel c are symmetric with respect to the white dashed diagonal line.

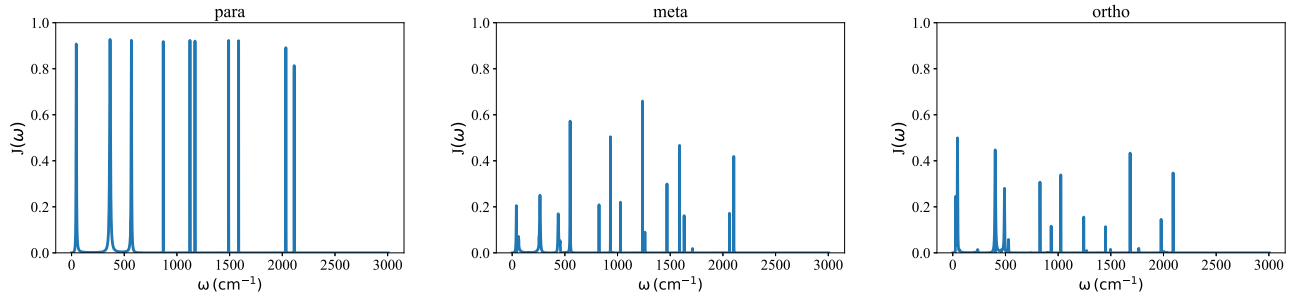

Figure 7. Frequency-resolved energy flux (arbitrary units) generated by driving one sulfur atom of a benzenedithiol molecule and evaluating the heat generation per unit time on the other sulfur taking friction $\gamma = 20$ cm^{-1} to affect the motion along the S−C bond, calculated according to eq 5.

examine, for more anharmonic systems, the effect of anharmonicity. Beyond such studies, it is of interest to examine the possibility of using interference as a tool for controlling heat conduction properties of different molecular structures.

APPENDIX: TRANSMISSION FUNCTIONS IN THE HARMONIC LIMIT

The quantum heat conduction shown in this Letter are obtained from the transmission function obtained from the Landauer

https://dx.doi.org/10.1021/acs.jpclett.0c00471
J. Phys. Chem. Lett. 2020, 11, 4261−4268

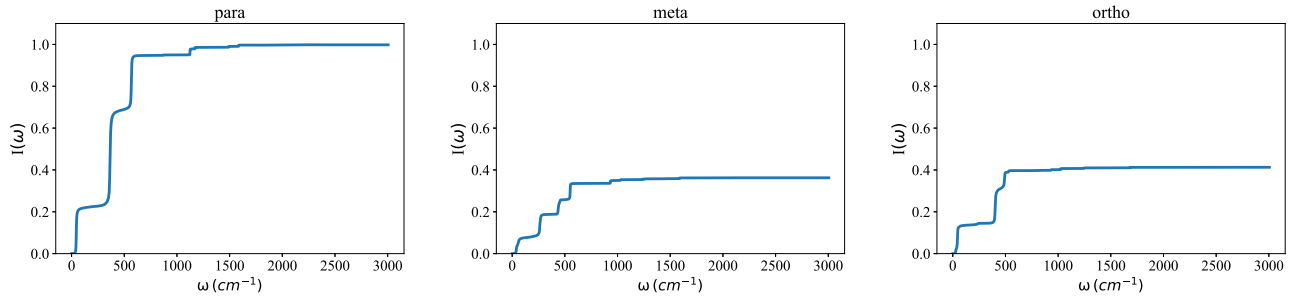

Figure 8. Integrals $I(\omega) = \int_0^{\omega} d\omega\, J(\omega)$ over the frequency-resolved heat fluxes of Figure 7, normalized by $I_{\text{para}}(3000\ \text{cm}^{-1})$ and displayed against ω for the three benzendithiol species.

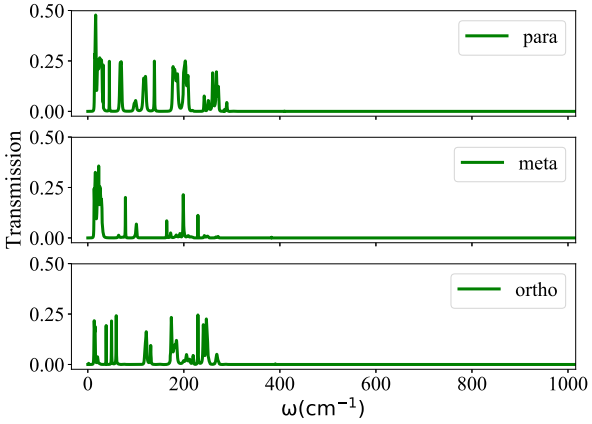

Figure 9. Quantum transmission coefficient for the para, meta, and ortho benzenedithiol structures between gold substrates, used to obtained the Landauer results near 300 K. Note that the transmission vanishes above the gold Debye frequency.

formula.[7,29,30] Transmission function for the para, meta, and ortho benzene structures between gold substrates about room temperatures are shown in Figure 9. Here we outline the way to calculate a classical equivalent as an intrinsic property of the molecular structure. Consider the molecular bridge segment (in our case the benzenedithiol molecule) as multiatom driven damped harmonic system defined by the equation of motion

$$\ddot{\mathbf{X}} = -\frac{1}{2}\mathbf{K}\mathbf{X} - \mathbf{G}\dot{\mathbf{X}} + \mathbf{A}(t) \tag{3}$$

where $\mathbf{X}$ is a vector of mass-weighted atomic deviations from equilibrium, $\mathbf{K}$ the Hessian matrix associated with the molecular force field, $\mathbf{G}$ a damping matrix, and $\mathbf{A}(t)$ a vector of externally imposed driving forces on the different atoms. We are interested in the particular situation in which periodic forces $\mathbf{A}(t)$ reduce to harmonic driving $\mathbf{A}\cos(\omega t)$ of the atom that in the corresponding junction is attached to one lead, while friction, not necessary isotropic, is imposed on the atom that in the corresponding junction is connected with the other lead. A one-dimensional cartoon is seen in Figure 10. In this one-dimensional case, $\mathbf{A}$ and $\mathbf{G}$ are

$$\mathbf{A}(t) = \mathbf{A}e^{i\omega t} = \begin{pmatrix} 0 \\ 0 \\ \vdots \\ a \end{pmatrix} e^{i\omega t}, \qquad \mathbf{G} = \begin{pmatrix} \gamma & 0 & \dots & 0 \\ 0 & 0 & \dots & 0 \\ \vdots & \vdots & \ddots & \vdots \\ 0 & 0 & \dots & 0 \end{pmatrix} \tag{4}$$

(the real part of the solution is to be used) and in the three-dimensional case the nonzero blocks correspond to the atom(s)

Figure 10. One-dimensional damped and driven harmonic chain.

that in the junction is(are) attached to the lead, taken in the present calculation to be the sulfurs. At long time all atomic displacements oscillate with the driving frequency $X_j(t) = x_j(\omega)\, e^{i\omega t}$ and the amplitudes x_j may be obtained from $\mathbf{x} = \left(-\omega^2\mathbf{I} + \frac{1}{2}\mathbf{K} + \mathbf{G}\right)^{-1}\mathbf{A}$. The dissipated energy flux (averaged over a period) is then obtained from

$$J(\omega) = \overline{\dot{\mathbf{X}}\cdot\mathbf{G}\dot{\mathbf{X}}} = \frac{1}{2}\omega^2\mathbf{x}\times\mathbf{G}\mathbf{x} \tag{5}$$

which is just $(1/2)\omega^2\gamma x_1{}^2$ in the one-dimensional example. In three dimensions, when the lead−molecule coupling involves a single molecular atom we take $\mathbf{x}\cdot\mathbf{G}\mathbf{x} = \sum_{k=1}^{3}\gamma_k x_{1k}$ to reflect possible anisotropy of the friction.

AUTHOR INFORMATION

Corresponding Author

Abraham Nitzan − *Department of Chemistry, University of Pennsylvania, Philadelphia, Pennsylvania 19104, United States; School of Chemistry, Tel Aviv University, Tel Aviv 69978, Israel;* orcid.org/0000-0002-8431-0967; Email: anitzan@sas.upenn.edu

Authors

Renai Chen − *Department of Chemistry, University of Pennsylvania, Philadelphia, Pennsylvania 19104, United States*

Inon Sharony − *School of Chemistry, Tel Aviv University, Tel Aviv 69978, Israel*

Complete contact information is available at: https://pubs.acs.org/10.1021/acs.jpclett.0c00471

Notes

The authors declare no competing financial interest.

ACKNOWLEDGMENTS

The research of A.N. is supported by the Israel-U.S. Binational Science Foundation, the German Research Foundation (DFG TH 820/11-1), the U.S. National Science Foundation(Grant No. CHE1665291), and the University of Pennsylvania.

REFERENCES

(1) Cahill, D. G.; Ford, W. K.; Goodson, K. E.; Mahan, G. D.; Majumdar, A.; Maris, H. J.; Merlin, R.; Phillpot, S. R. Nanoscale thermal transport. *J. Appl. Phys.* **2003**, *93*, 793−818.

https://dx.doi.org/10.1021/acs.jpclett.0c00471
J. Phys. Chem. Lett. 2020, 11, 4261−4268

(2) Cahill, D. G.; Braun, P. V.; Chen, G.; Clarke, D. R.; Fan, S.; Goodson, K. E.; Keblinski, P.; King, W. P.; Mahan, G. D.; Majumdar, A.; Maris, H. J.; Phillpot, S. R.; Pop, E.; Shi, L. Nanoscale thermal transport. II. 20032012. *Appl. Phys. Rev.* **2014**, *1*, No. 011305.
(3) Leitner, D. M. Quantum ergodicity and energy flow in molecules. *Adv. Phys.* **2015**, *64*, 445−517.
(4) Dubi, Y.; Di Ventra, M. *Colloquium*: Heat flow and thermoelectricity in atomic and molecular junctions. *Rev. Mod. Phys.* **2011**, *83*, 131−155.
(5) Li, N.; Ren, J.; Wang, L.; Zhang, G.; Hänggi, P.; Li, B. *Colloquium*: Phononics: Manipulating heat flow with electronic analogs and beyond. *Rev. Mod. Phys.* **2012**, *84*, 1045−1066.
(6) Rubtsova, N. I.; Rubtsov, I. V. Vibrational Energy Transport in Molecules Studied by Relaxation-Assisted Two-Dimensional Infrared Spectroscopy. *Annu. Rev. Phys. Chem.* **2015**, *66*, 717−738.
(7) Segal, D.; Agarwalla, B. K. Vibrational Heat Transport in Molecular Junctions. *Annu. Rev. Phys. Chem.* **2016**, *67*, 185−209.
(8) Cui, L.; Miao, R.; Jiang, C.; Meyhofer, E.; Reddy, P. Perspective: Thermal and thermoelectric transport in molecular junctions. *J. Chem. Phys.* **2017**, *146*, No. 092201.
(9) Rubtsov, I. V.; Burin, A. L. Ballistic and diffusive vibrational energy transport in molecules. *J. Chem. Phys.* **2019**, *150*, No. 020901.
(10) Cui, L.; Hur, S.; Akbar, Z. A.; Klöckner, J. C.; Jeong, W.; Pauly, F.; Jang, S.-Y.; Reddy, P.; Meyhofer, E. Thermal conductance of single-molecule junctions. *Nature* **2019**, *572*, 628−633.
(11) Hansen, T.; Solomon, G. C. When Conductance Is Less than the Sum of Its Parts: Exploring Interference in Multiconnected Molecules. *J. Phys. Chem. C* **2016**, *120*, 6295−6301.
(12) Hansen, T.; Solomon, G. C.; Andrews, D. Q.; Ratner, M. A. Interfering pathways in benzene: An analytical treatment. *J. Chem. Phys.* **2009**, *131*, 194704.
(13) Solomon, G. C.; Andrews, D. Q.; Van Duyne, R. P.; Ratner, M. A. When Things Are Not as They Seem: Quantum Interference Turns Molecular Electron Transfer Rules Upside Down. *J. Am. Chem. Soc.* **2008**, *130*, 7788−7789.
(14) Solomon, G. C.; Andrews, D. Q.; Hansen, T.; Goldsmith, R. H.; Wasielewski, M. R.; Van Duyne, R. P.; Ratner, M. A. Understanding quantum interference in coherent molecular conduction. *J. Chem. Phys.* **2008**, *129*, No. 054701.
(15) Solomon, G. C.; Herrmann, C.; Hansen, T.; Mujica, V.; Ratner, M. A. Exploring local currents in molecular junctions. *Nat. Chem.* **2010**, *2*, 223−228.
(16) Garner, M. H.; Li, H.; Chen, Y.; Su, T. A.; Shangguan, Z.; Paley, D. W.; Liu, T.; Ng, F.; Li, H.; Xiao, S.; Nuckolls, C.; Venkataraman, L.; Solomon, G. C. Comprehensive suppression of single-molecule conductance using destructive σ-interference. *Nature* **2018**, *558*, 415−419.
(17) Garner, M. H.; Solomon, G. C.; Strange, M. Tuning conductance in aromatic molecules: Constructive and counteractive substituent effects. *J. Phys. Chem. C* **2016**, *120*, 9097−9103.
(18) Manrique, D. Z.; Huang, C.; Baghernejad, M.; Zhao, X.; Al-Owaedi, O. A.; Sadeghi, H.; Kaliginedi, V.; Hong, W.; Gulcur, M.; Wandlowski, T.; Bryce, M. R.; Lambert, C. J. A quantum circuit rule for interference effects in single-molecule electrical junctions. *Nat. Commun.* **2015**, *6*, 6389.
(19) Markussen, T.; Stadler, R.; Thygesen, K. S. The relation between structure and quantum interference in single molecule junctions. *Nano Lett.* **2010**, *10*, 4260−4265.
(20) Medrano Sandonas, L.; Rodríguez Méndez, Á.; Gutierrez, R.; Ugalde, J. M.; Mujica, V.; Cuniberti, G. Selective Transmission of Phonons in Molecular Junctions with Nanoscopic Thermal Baths. *J. Phys. Chem. C* **2019**, *123*, 9680−9687.
(21) Hu, S.; Zhang, Z.; Jiang, P.; Chen, J.; Volz, S.; Nomura, M.; Li, B. Randomness-Induced Phonon Localization in Graphene Heat Conduction. *J. Phys. Chem. Lett.* **2018**, *9*, 3959−3968.
(22) VanGessel, F.; Peng, J.; Chung, P. W. A review of computational phononics: the bulk, interfaces, and surfaces. *J. Mater. Sci.* **2018**, *53*, 5641−5683.
(23) Chen, R.; Craven, G. T.; Nitzan, A. Electron-transfer-induced and phononic heat transport in molecular environments. *J. Chem. Phys.* **2017**, *147*, 124101.
(24) Moghaddasi Fereidani, R.; Segal, D. Phononic heat transport in molecular junctions: Quantum effects and vibrational mismatch. *J. Chem. Phys.* **2019**, *150*, No. 024105.
(25) Li, Q.; Strange, M.; Duchemin, I.; Donadio, D.; Solomon, G. C. A strategy to Suppress Phonon Transport in Molecular Junctions Using π-Stacked System. *J. Phys. Chem. C* **2017**, *121*, 7175−7182.
(26) Markussen, T. Phonon interference effects in molecular junctions. *J. Chem. Phys.* **2013**, *139*, 244101.
(27) Pronk, S.; Páll, S.; Schulz, R.; Larsson, P.; Bjelkmar, P.; Apostolov, R.; Shirts, M. R.; Smith, J. C.; Kasson, P. M.; van der Spoel, D.; Hess, B.; Lindahl, E. GROMACS 4.5: a high-throughput and highly parallel open source molecular simulation toolkit. *Bioinformatics* **2013**, *29*, 845−854.
(28) Rappe, A. K.; Casewit, C. J.; Colwell, K. S.; Goddard, W. A.; Skiff, W. M. UFF, a full periodic table force field for molecular mechanics and molecular dynamics simulations. *J. Am. Chem. Soc.* **1992**, *114*, 10024−10035.
(29) Dhar, A.; Roy, D. Heat Transport in Harmonic Lattices. *J. Stat. Phys.* **2006**, *125*, 801−820.
(30) Segal, D.; Nitzan, A.; Hänggi, P. Thermal conductance through molecular wires. *J. Chem. Phys.* **2003**, *119*, 6840−6855.
(31) Sharony, I.; Chen, R.; Nitzan, A. Stochastic Simulation of Nonequilibrium Heat Conduction in Extended Molecular Junctions. Submitted for publication.
(32) Torii, D.; Nakano, T.; Ohara, T. Contribution of inter- and intramolecular energy transfers to heat conduction in liquids. *J. Chem. Phys.* **2008**, *128*, 044504.
(33) Altman, D. G.; Bland, J. M. Standard deviations and standard errors. *BMJ. (Clinical research ed.)* **2005**, *331*, 903.
(34) YALIRAKI, S. N.; RATNER, M. A. Interplay of Topology and Chemical Stability on the Electronic Transport of Molecular Junctions. *Ann. N. Y. Acad. Sci.* **2002**, *960*, 153−162.
(35) Rai, D.; Hod, O.; Nitzan, A. Circular Currents in Molecular Wires. *J. Phys. Chem. C* **2010**, *114*, 20583−20594.

https://dx.doi.org/10.1021/acs.jpclett.0c00471
J. Phys. Chem. Lett. 2020, 11, 4261−4268

https://dx.doi.org/10.1021/acs.jpclett.0c00471
J. Phys. Chem. Lett. 2020, 11, 4261−4268